Current Collection in a Spacecraft Wake; Laboratory and Computer Simulations

Chung Chan, Jim Browning, Steve Meassick
Department of Electrical and Computer Engineering
and Center for Electromagnetics Research
Northeastern University, Boston, MA 02115

M.A. Morgan
AMPTEK Inc.
6 DeAngelo Drive, Bedford, MA 01890

David L. Cooke, C. L. Enloe
Air Force Geophysical Laboratory
Hanscom AFB, MA 01731

Maurice F. Tautz
Radex Incorporated
3 Preston Ct., Bedford, MA 01730

I. Introduction

The current-voltage (IV) characteristic of a charged object in the wake of another, larger body in Low Earth Orbit (LEO) is an issue that is relevant to spacecraft design and operation. Deep in the wake of a platform that is possibly thousands of Debye lengths across, the plasma density and currents will be reduced to a fraction of their values in the ambient stream creating conditions where high voltage power equipment could be hidden from the plasma or an astronaut on EVA in polar orbit might become charged by auroral electrons. The wake charging problem, as it is called, is difficult to analyze because plasma currents will remain small until the object potential is sufficient to pull charged particles from the dense plasma stream across an ion void and, in the case of ion collection, overcome a significant angular momentum barrier. The wake charging problem has received some attention to date, (Jongeward, 1986) but the use of the theoretical tools used in that study was somewhat idealized, and no in-situ measurements were available to validate the predictions.

We have begun a series of laboratory experiments to study the wake charging of a very negatively biased body. In the present experiment, an ion thruster is used to produce a flowing plasma in a large vacuum chamber. A 10 *cm* diameter aluminum disk is inserted into this plasma to produce a wake. A smaller spherical probe is mounted on an XY table and inserted into the disk's wake where its (ion) IV characteristic can be measured as a function of location and potential. This "small beam in a large chamber" approach is adopted to minimize the effects of charge exchange ions and the chamber walls.

A common and reasonable goal of a laboratory plasma simulation is to provide scientific and engineering data that can be *scaled to space*. That sort of approach is limited in this problem because of the size of the parameter space that determines the current, I. The minimum set of dimensionless parameters are expressed,

$$I = I\,(\Phi_p, \Phi_d, R_p, R_d, M, D_{pd})$$

where $\Phi = eV/kT$, e is the electron charge, k is Boltzman's constant, T is the plasma temperature, V is the potential on both the disk V_d and the probe V_p, and $M = Velocity / \sqrt{2kT/m}$ is the ion Mach speed of the flow. The R's are radii of the disk and probe normalized by the Debye length, $\lambda_D = e\sqrt{N/kT\varepsilon_0}$ and $D_{pd} = d/\lambda_D$ is the normalized separation distance. Certainly, if this list is complete, and each of the parameters are identical between two configurations, the currents should scale as well. Less trivial is the sort of scaling where one asks "how does *this* scale with *that*?", which is equivalent to knowing the physical law relating *this* and *that*, but with a minimum of 6 parameters, such laws are actually large families of relations that would be difficult to use even if known. One way to enhance the scalability of the laboratory results is to develop and/or apply a suitable computer model that can reproduce the laboratory results, and provide predictions for problems that are not parametrically identical to what was studied in the lab.

The Air Force Geophysics Laboratory has a 3D computer code, POLAR (*P*otential of *L*arge *O*bjects in the *A*uroral *R*egion: Cooke, 1985) to address this and other LEO spacecraft-plasma interactions. POLAR is a Poisson-Vlasov code that was written to model the interactions of large spacecraft with the LEO plasma and is somewhat specific to the space environment. POLAR can accept chamber plasma parameters, but cannot account for many other differences between chamber and space conditions, such as ion beam anisotropy and divergence, and thermo-electric (wall) effects.

A second computer code, MACH, has also been useful in this investigation. MACH (*M*esothermal *A*uroral *CH*arging: Tautz, 1987) is a [2D-3V] axisymmetric program that can perform both chamber and space simulations with an approach that differs significantly from POLAR.

In this paper, we describe the laboratory experiment and compare our results with both the MACH and the POLAR codes. We have found reasonable agreement in the results of the experimental and two numerical simulations. MACH produced a close match on structure of both 'ambient' and the high potential region close to the probe. POLAR's predicted current-voltage curve for the probe reproduces many of the curve characteristics. There does, however, appear to be secondary current effects that neither code predicted.

II. Laboratory Experiment

Our experiments were performed in a large cylindrical vacuum chamber with a diameter of 1.7m and a length of 1.7m. An ion gun (a three-grid Kaufman thruster) produces a flowing Argon plasma into which an aluminum disk of radius $b = 10\,cm$ is inserted. A stainless steel spherical probe with radius $a = 0.5\,cm$ is placed behind the disk along the axis of the disk and the ion gun. The separation between the ion gun and the disk is approximately 35 to 40 cm while the separation between the disk and the spherical probe can be varied from 1 to $15\,cm$. The configuration of the chamber simulation viewed from the top and the side, is depicted in Fig. 1.

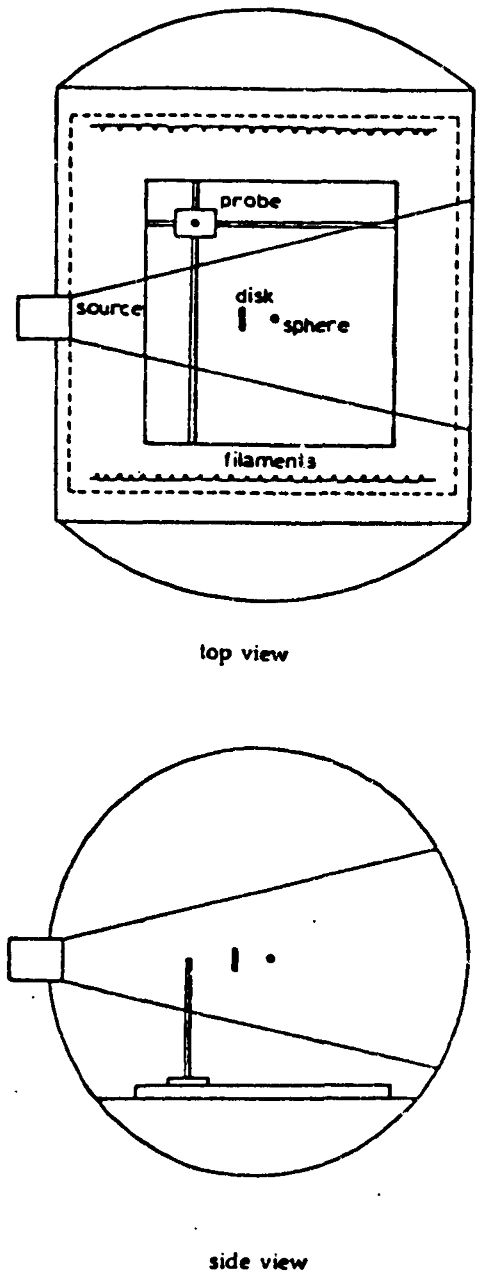

Figure 1. Configuration of the Chamber simulation

Various Langmuir probes, emissive probes and retarding potential analyzers (RPA's) can be mounted on a XYZ table to perform three dimensional mapping of electron and ion current densities, temperatures, and plasma potential. For the ion current collection experiment, singly charged ions are accelerated across a $100V$ net potential drop to produce the flowing stream, then neutralized by electrons from a hot filament located near the last ion electrode. At a typical ion current of $I_b = 32\,mA$ and a neutralizing electron current of $I_n = 35\,mA$, the beam energy is measured by the RPA to be $90\,eV$ with a thermal energy width parallel to the beam of $T_{//} = 10\,eV$. The beam width (FWHM) is $40\,cm$ at the location of the disk and the corresponding plasma density is $N_p = 10^8\,cm^{-3}$. Using this density and the $T_{//} = 10\,eV$ produces a Debye length, $\lambda_D = 0.2\,cm$, making the disk about 42 λ_D across. The background pressure of the chamber is normally in the 10^{-7} *Torr* range and increases to 1 to $2x\ 10^{-6}$ *Torr* when the ion gun is operated. Less than one percent of the ion species are found to be charge exchange cold ions with temperature less than $1\,eV$. The electron temperature is in the range of $5 - 8\,eV$, and the ion Mach number, $M \geq 3$. Near the beam center, the average plasma potential is 2 to 4 volts above ground which is in agreement with the plasma potential distributions calculated by the MACH code (see section *VI*).

In the present experiment, the sphere is biased from $V_p = 0$ to $-10kV$ and the collected ion current is measured with the circuit shown in Fig. 2. A current limiting resistor $R = 1MW$ is employed in the circuit to prevent current run away at high negative voltage with unexpected pressure rise due to arcing. The value of the current limiting resistor is chosen so that the I-V curve will not be distorted at its high-current end.

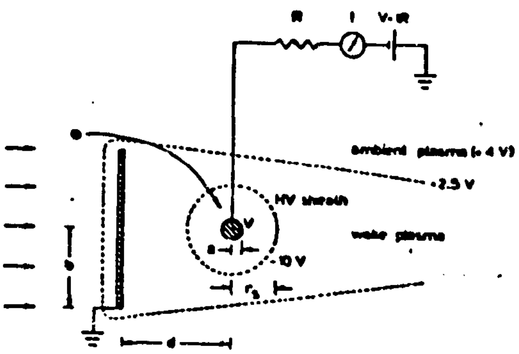

Figure 2. Schematic for Current Collection in the Wake

An emissive probe is used to measure the plasma potential around the charged sphere and in the wake of the disk. A small tungsten filament (1 *mil* in diameter) is heated to emission with a current of approximately $3\,mA$. A sweep generator is then used to vary the filament bias over a range from -30 to $30V$. When the probe is biased more negatively than the plasma potential, the probe will emit. This emission can be detected by measuring the voltage across a resistor to ground. As the bias voltage is swept from negative to positive, the emission will approach zero at the plasma potential. Using this technique, the potential around the charged sphere is measured with an error of $\pm 0.2\,V$. The probe has a spatial resolution of $0.5\,cm$.

III. Observations

In Fig. 3, we show the ion current collected by the sphere as a function of the sphere bias voltage when the sphere is at a distance of 2, 4 and $10\,cm$ behind the disk which is at ground potential. The current saturation at high bias voltages is a real phenomenon and not an artifact due to the limiting resistor. The ion current increases almost vertically at $-2.5kV$ when the operating neutral pressure is increased to $2x\,10^{-5}\,torr$. At such high pressure, the high voltage can produce significant ionization which leads to current run away.

Upon careful examination of data such as Fig. 3, the following phenomena were observed: (1) There is a threshold voltage, V_{tr}, at which a rapid increase of ion current to the sphere is observed; (2) V_{tr} increases as the separation, d, between the disk and the sphere decreases (e.g. $V_{tr} = -2.2\,kV$ at $d = 2\,cm$ and $V_{tr} = -1.6\,kV$ at $d = 10\,cm$); and (3) The magnitude of collected ion current increases as d increases.

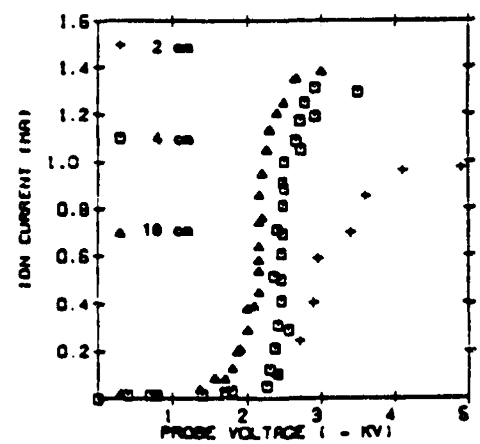

Figure 3. Measured Current collection versus Separation

Another observation, not obvious from Fig. 3, is an ion current relaxation at successive sphere voltage steps, the relaxation time t_o being typically a few minutes. The data presented in Fig. 3 is obtained by waiting 10 minutes between each voltage step. Data obtained in this fashion was reproducible from day to day and with only minor variations up to a few months during the course of this experiment.

However, swept I-V curves with each voltage step taken less than a few minutes apart (as in the case of a space experiment) may be problematic in the high voltage regime. The current fluctuations may be a result of reaching equilibrium between various processes (e.g. secondary electron emission, sputtering and of outgassing from the surface of the sphere) as the voltage increases by 20 to $50\,V$ (a typical voltage step in our experiment). It may also be affected by the high voltage sheath capacitance in series with the current collecting circuit and the limiting resistor, R.

The collection of ions in the wake of a small object, as shown in Fig. 3, can be understood by studying the high voltage sheath in the wake of the disk. In Fig. 4, we show the three-dimensional plasma potential contours in the wake when $d = 5cm$ and the bias voltage on the sphere is $-5kV$. Because of the strong potential gradient near the sphere, the approximately 250 data points were taken with as fine a spatial resolution as possible (~0.5 cm). As the data was taken and the potential variation was observed, the mesh was varied accordingly. Therefore, most of the data points were taken near the sphere and the disk where the strongest gradients occurred. However, when the plasma potential was less than $-10\,V$, the emission of the probe was so small that accurate estimates of the potential were difficult. In addition, heating the probe to higher emission greatly reduced the probe's lifetime. Hence, the minimum potential measured was $-10\,V$ as indicated by the inner contour. To insure consistent measurements, the filament current was held constant through the entire data set.

The high voltage sheath is approximately spherical and bounded by the wake of the disk. If we assume that the $-10\,V$ equipotential contour represents the sheath edge, the sheath thickness (radius) d_s increases from 2 to $4\,cm$ when the bias voltage V_p varies from $-1\,kV$ to $-5\,kV$.

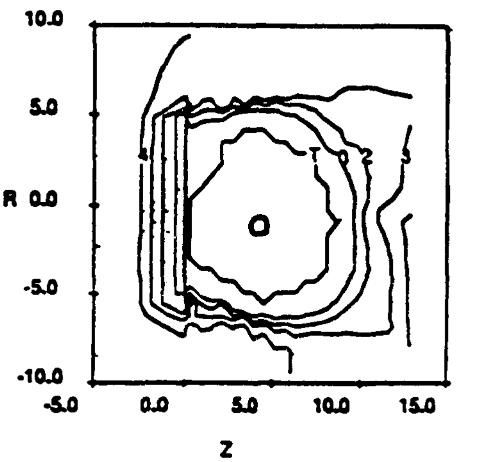

Figure 4. Measured Potential Contours for -5 KV probe Bias and separation d = 5 cm. Voltage Contour levels are:
-10.0 = T , 0.0 = 0,
2.0 = 2 , 3.0 = 3,
4.0 = 4

The most obvious and significant results of the chamber tests is the observation of a sudden onset of ion current collection once a threshold voltage is attained. The magnitude of this threshold voltage is seen to vary with the separation between disk and sphere.

IV. Analysis

Our objective in this experiment, is to understand the magnitude and the morphology of the observed I-V curve, and to validate the computer models. Our analysis is based on the presumed interplay between three effects: sheath formation in the wake, conservation of angular momentum within the sheath, and the effect of weak non-radial fields outside of the sheath.

The electric fields reach saturated strength when the the space charge sheath that the probe would attain outside of the wake begins to exceed the dimension of the wake. We claim that a sheath extending beyond the disk is a necessary but not sufficient condition for the current collection voltage threshold. Using the Langmuir-Blodgett (Langmuir, 1924) spherical sheath model, the sheath thickness can be expressed as (Parker, 1980):

$$d_s = a\left\{\frac{1}{2}+\left[\frac{1}{4}+\frac{d_{cl}}{a}\right]^{1/2}+0.052\frac{d_{cl}}{a}\right\} \quad (1)$$

where a = 0.5 cm is the radius of the sphere and

$$d_{cl} = 1.26\lambda_D\left[\frac{eV_p}{kT}\right]^{3/4} \quad (2)$$

where d_{cl} is the thickness of the planar Child-Langmuir sheath and λ_D is the Debye length. For our experiment, using $\lambda_D = 0.23\,cm$ and $T = T_{//} = 10\,eV$ gives $d_s = 3.8\,cm$ at $V_p = -2kV$, which is a bit less than the disk radius $b = 5\,cm$. $T = T_{//} = 10\,eV$ is, however, an overestimate of the appropriate temperature, since at $V_p < V_{tr}$, it is $T_\perp$ that specifies the flux into the wake, and for an idealized beam, $T_\perp$ can be undefined. The temperature that produces $d_s = b$ is $T = 5.5\,eV$, which might be reasonable. The value of this portion of our analysis is to identify the interaction of sheath and wake, and what is required of numerical tools to properly account for actual configurations.

The symmetry of the chamber experiment suggests that conservation of angular momentum will be another constraint on current collection. Letting the radius of the disk define a minimum impact parameter necessary for collection of the streaming ions by the sphere, the angular momentum, L_i, of ions relative to the sphere is initially,

$$L_i = b\left[2\frac{E_b}{m_i}\right]^{1/2} \quad (6)$$

and at the surface, biased to V_{tr}

$$L_f = a\left[2\frac{(E_b + eV_{tr})}{m_i}\right]^{1/2} \quad (7)$$

Setting these equal, conservation requires that:

$$V_{tr} = \frac{E_b(b^2 - a^2)}{e\,a^2} = 8.9\,kV \quad (8)$$

using $E_b = 90\,eV$, $b = 5\,cm$, and $a = 0.5\,cm$. This voltage threshold is significantly higher than what is measured. Furthermore, the angular momentum argument predicts no dependence on the separation between the disk and the sphere. This arises from the implicit assumption that the forces acting on the ion are spherically radial. While this is true in and near the sheath (that is, for most of the time the ion is accelerated), it is untrue near the edge of the disk where the electric field is more cylindrically radial as can seen in Fig. 4, and 9. The electric field structure is such that an ion passing near the edge of the disk will be subjected to an impulse directed cylindrically radially inward. Suppose that an ion is turned though an angle θ at the edge. As Fig. 5 illustrates, it now approaches the sphere with an effective impact parameter b' that is less than b. This effective impact parameter may be shown to be:

$$b' = b\cos\theta - d\sin\theta \quad (9)$$

Substituting b' for b in Eq. 8 and solving for V as a function of d gives the results shown in Fig. 6, for $a = 0.5\,cm$ and $b = 5\,cm$. Qualitatively, the experiment results are predicted; as the separation d increases, the threshold voltage decreases.

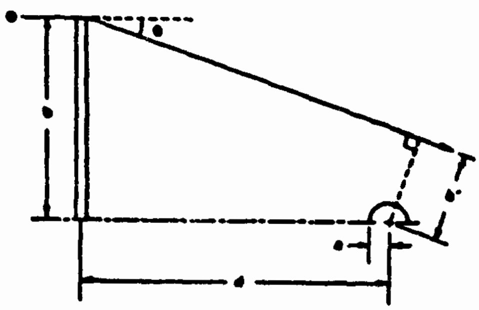

Figure 5. Angular Momentum for Ions in the Wake

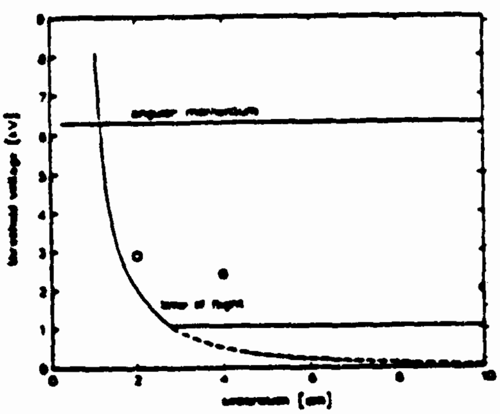

Figure 6. Calculated Theshold Voltage Versus Probe Separation

The measured threshold voltages are also indicated on the figure. The measurements indicate that if the modified angular momentum criterion is correct, the deflection of the ions at the edge must be between approximately 10 and 25 degrees. We check this by making the assumption that the electric field near the edge of the disk is on the order of $kT_{\perp}/e\,\lambda_D$. Applying a time of flight analysis, where the length of the interaction region is L, the angular deflection is given by

$$\theta = \tan^{-1}\left(\frac{V_{\perp}}{V_{//}}\right) = \tan^{-1}\left(\frac{LkT}{\lambda_D\, 2E_b}\right) \quad (10)$$

Using $\lambda_D = 0.23\,cm$, $kT_{\perp}/e = 4\,V$, $E_b = 90\,eV$ and $L = 4\,cm$, Eq. 10 predicts $\theta = 20°$.

The angular momentum criterion provides another necessary but not sufficient bound on the threshold voltage required to attract ions to a small body in the wake of a larger body. The current collection is however, quite sensitive to the details of the field structure, especially near the edge of the shadowing body.

V. Enhanced Secondary Emission

The magnitude of the ion current collected by the sphere would also depend on several atomic processes occurring on the surface of the sphere. The first process is the sputtering of the surface by the energetic ions. Since the the sphere is biased at very negative potential, sputtered ions or back scattered ions off the sphere would be repelled back to the sphere by the ion sheath. The second process is emission of secondary electrons and negative ions which enhance the current to the sphere.

Enhanced secondary emission has been observed from a strongly negatively biased sphere inserted in an ion beam. Preliminary results indicate that this emission may increase the apparent ion current collected by the sphere by a factor of 2 - 3.

The enhanced secondary current was observed by placing in a beam plasma the same stainless steel sphere (0.5 cm radius) as was used in wake experiment just described. For this measurement, the sphere was surrounded with a grounded spherical wire mesh, having a radius of 4.0 cm. The wire mesh ensured that the ion flux being accelerated into the negatively biased sphere was constant and independent of the bias voltage. In this configuration, the sphere was biased over the same range of negative potential as before, and current recorded. This current is the sum of the beam ion current and any secondary currents being emitted by the sphere or mesh. Fig 7. shows the amount of current collected by the sphere as a function of the bias voltage. It can be seen that the current rapidly rises for low bias voltages, rises more slowly just past -500 V, but rises more rapidly again at bias voltage greater than -2000 V. This current profile is consistent with the picture of beam ion current saturating near -500 V, and a secondary process providing current enhancement for more negative voltage. For bias potentials above -2000 V the rapid increase in the current collection would seem anomalous since all ions are already being collected by the biased sphere and the grounded spherical wire mesh prevents the expansion of the ion collection sheath.

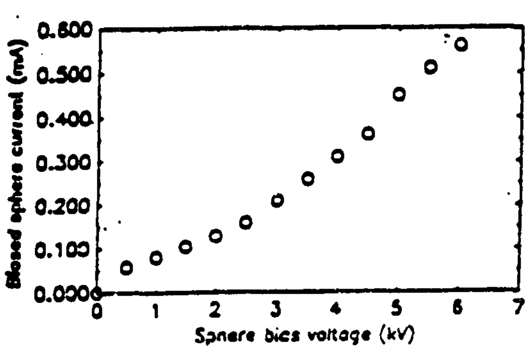

Figure 7. Measured Sphere Current Versus Bias Voltage

In order to ascertain that this increase in current is due to the emission of secondary particles, a gridded particle energy analyzer was placed at a radius of 5.4 cm from the biased sphere and looking radially inward. The energy analyzer was biased to reject all ions and electrons with an energy of less than 70 eV, which is higher than the beam energy of 20 eV, but less than the energy of a negative particle originating from the biased sphere surface. It was noted that the amount of current collected by the energy analyzer is small until the sphere is biased to approximately -1500, after which it increases rapidly. This is the same voltage at which the current to the sphere starts to increase again.

By moving the energy analyzer azimuthally around the biased sphere in the plane of the beam the total amount of secondary current can be calculated. This amounts to approximately 50% of the total current collected by the biased sphere when the bias is set at -4000 V. This compares favorably with the amount of current expected if one extrapolates the saturation current of the biased sphere to -4000 V. Both of these measurements indicate that the secondary current is comparable to the primary ion current and even exceeds it for sphere bias voltages more negative than -4000 V.

The energy distribution of the secondary particles was also measured. Fig. 8 shows the amount of current collected by the energy analyzer as a function of the repeller voltage. The sphere bias was set to -4000 V. The sharp cutoff of the analyzer current above 4000 V indicates that all of the particles coming from the biased sphere have an energy of 4000 eV. If the electrons (or ions) were born anywhere but on the sphere, as in the ionization of neutral gas in the gap between the sphere and mesh, a broader particle energy distribution would result.

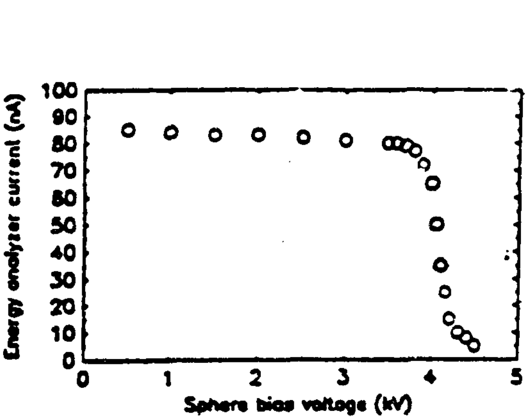

Figure 8. Measured Energy Analyser Current Versus Bias Voltage

The anticipated secondary electron yield for ion bombardment of stainless (composition uncertain) is about 10 to 20% over most of our energy range. The sputtering yield, however, of the constituent stainless metals under Argon bombardment rises to values greater than 1 or 2. This points to sputtering as a possible contributor to our high secondary current observations. Whether ions or electrons actually carry the secondary current remains to be determined.

VI. The MACH Code

The MACH (Tautz, 1987) code, derived from the earlier program TDWAKE (Parker, 1976), solves the Poisson-Vlasov equations self-consistently on a discrete cylindrical (R,Z) mesh. MACH solves the Poisson equation by simple first order differencing and point successive over relaxation with a space charge iteration similar to that of POLAR. A reversed trajectory "inside-out" method is used to calculate densities and currents by employing the result of Liouville's Theorem, "The distribution function, $f = f(v,r)$, is constant along a particle trajectory". Thus we build up and integrate f to obtain densities and higher moments at each node in the grid, by tracing reverse trajectories to where f is known. This makes the specification of charged particle boundary conditions quite straght forward. This method of obtaining densities has a fundamental appeal, since there are no approximations beyond collisionless-ness. There is a presumption of trajectory accuracy, and that f can be sampled with sufficient resolution. We have been able to improve the resolution and efficiency of the method by employing a velocity space topology search, VSTS. At each node, trajectories are "launched" initially at coarse intervals. Intervals are repeatedly halved on subsequent passes, if inspection of f on the previous interval indicates that a region needs greater resolution. VSTS has significantly extended the high voltage capability of the inside-out method, however velocity space resolution still sets the high voltage limits of the method.

The wall boundary conditions for the chamber simulations are zero potential and no emission. The ion gun is represented as a zero potential boundary emitting a a drifting Maxwellian ion distribution. Electrons from the neutralizing filement are represented by an isotropic Maxwellian source. All particles incident on the probe, the disk or the walls are assumed to be absorbed.

Possibly the most fundamental difference between chamber and space plasma is the electron population and in particular how trapped electrons are modeled. In space, a collisionless (Vlasov) plasma has $n(e) = n(i)$, and $j(e) >> j(i)$ whereas our plasma source produces $j(e) = j(i)$ and $n(e) << n(i)$. Modeling the plasma with only Vlasov electrons results in violently unphysical space charge instability. MACH has a trapped electron model in which the ion space charge creates a potential well for electrons, of depth Φ. The code assumes that electrons scatter into this well and establish an isotropic equilibrium, with a temperature equal to the Vlasov electrons.

For comparison with this experiment MACH simulations were done with the front disk at zero potential and the sphere biased to $-1, -3$ and $-5KV$. The separation distance between the disk and the probe was taken to be $d = 5\ cm$. The potential contours for the $-5KV$ case are shown in Figure 9. It can be seen that the MACH solutions and the measurements both consist of an approximatley spherical region of high negative potential centered on the probe which decreases through zero into regions of positive potential where trapped electrons balance the source ions.

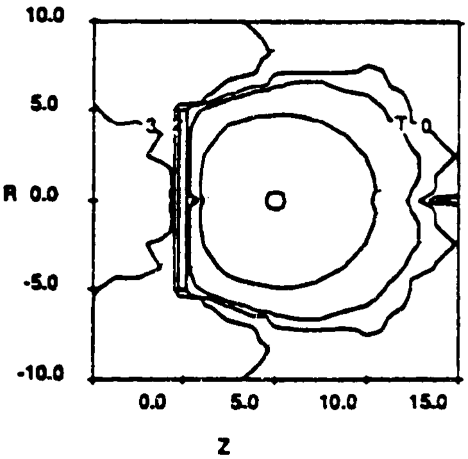

Figure 9. MACH Code Simulation of Potentials for -5 KV probe Bias and separation of d = 5 cm
Voltage Contour levels are:
-10.0 = T , 0.0 = 0,
2.0 = 2 , 3.0 = 3,
4.0 = 4

We have performed experiments and Mach simulations of the ion gun plasma without the disk or the spherical probe. For our beam, both experiment and simulation show a maximum positive space potential of about 4 *Volts* with good agreement on the distribution of potential throughout the beam region. This can also be observed on the edges of Figures 4 and 9, although with the disk and biased probe, the agreement near the probe is not as good as without.

The probe currents predicted by MACH are shown in Fig. 12. That these are less than the experimental or POLAR currents is expected. In the case of the experiment the as yet unquantified secondary emission effects can lead to a large increases in current and secondary emission is not modeled in MACH.

VII. The POLAR Code

POLAR is a self-consistent three dimensional Poisson-Vlasov code, that provides steady state solutions by iterating between potential (Poisson) and density (Vlasov) solutions on a cubical mesh. A versatile set of building elements can be combined to form complex objects with a variety of surface materials and electrical connections. A surface charging module can be added to the iteration to provide the spacecraft charging response to both natural and induced charge drivers. The Poisson solver uses a finite element conjugate gradient method, with a unique technique of filtering charge densities to suppress grid noise, and produce stable solutions. POLAR calculates particle densities by a method that divides space into (one or more) sheath and non-sheath regions separated by a sheath edge(s). External to sheath regions, densities are determined by geometric ray tracing with first order electric field corrections. This approach has been shown to correctly predict wake formation about the Space Shuttle Orbiter (Murphy et.al., 1987). Internal to the sheath, POLAR tracks ions and/or electrons to obtain densities. The POLAR method of particle tracking begins at a sheath edge, located as an equi-potential, near kT. External to this surface the plasma distribution is presumed to be Maxwellian with possible flow. Assuming a spherical r^{-2} potential variation outside of the sheath allows one to use the usual constants of motion and determine the flux and entry velocity of ions which are assigned to a super-particle and tracked. Densities are determined from the time spent in each volume element, and surface currents from their final deposition. When particles are repelled, their density is assumed to be Boltzmann.

POLAR was used to simulate the chamber experiment, using an octagonal disk, 9 grid units across, and a single unit cube for the probe. This is the minimum resolution that could be used, but higher resolution models indicated that it was adequate. Since POLAR does not trace trajectories outside of the sheath, the finite particle beam and walls could not be modeled. The Argon plasma input parameters were $N_e = 10^8\,cc^{-1}$, $kT = 10\,eV$ and the ion Mach number $M = 3$, The mesh spacing was $1.1\,cm$. corresponding to a Debye length of $\lambda_D = 0.23\,cm$, so that the disk was $42\,\lambda_D$ across. The front disk was held at a bias of $V_d = -1.0\,Volt$, and the probe voltage was swept from $V_p = -0.5$ to $-5.5\,kV$ in a series of runs.

A two dimensional cut through the -5 kV simulation is shown in Fig. 10, illustrating disk, probe, sheath and additional equipotential contours. We note that there are no positive potential contours which is reasonable since POLAR does not model the trapped electron population. Also shown in the plot are three out of the approximately 2000 trajectories traced by POLAR. Two of these enter the sheath very near the disk and have sufficiently little angular momentum to be collected. One trajectory missed the probe and has begun to orbit. It has been truncated for the figure only. These psuedo-trapped particles pose great difficulty for any steady state calculation, since they continue to contribute space charge as they orbit indefinitally. In the next Poisson solution, enough of this charge will cause the sheath to contract and exclude many of the psuedo-trapped orbits in the next current cycle. This may be controlled numericaly, and in POLAR, the orbit count is reduced untill the cycle to cycle current fluctuations are reasonable. Although this phenomenon is numerical, it does however point to the possibility of oscillations on the ion time scale.

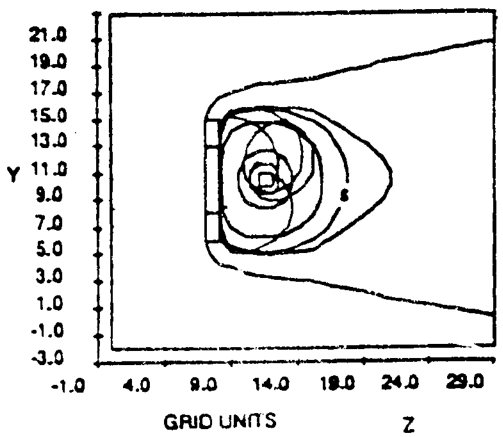

Figure 10. POLAR Code Potentials and Trajectories for -5 KV Probe Bias
Voltage Contour levels are:
-3000.0 , -1000.0
-100.0 , -20.0 = S
-10.0 , -1.0

The results of the complete suite of POLAR chamber runs are summarized in Fig. 11, where in addition to the voltage sweep, the separation distance between probe and disk was varied through values of $d = 2.7, 3.8$ and $4.9\ cm$. The [illegible] represent the degree of [illegible] fluctuation.

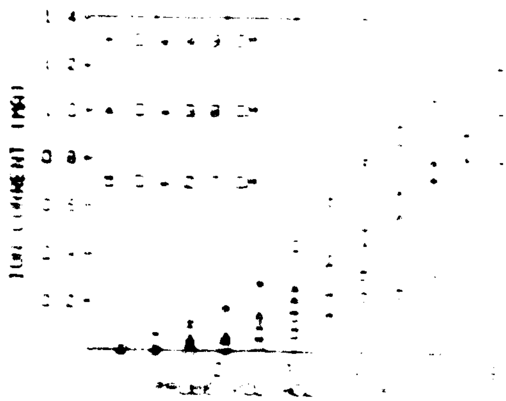

Figure 11. POLAR Code Simulation of [illegible] Current

The comparison between these results and the chamber measurements are better than expected considering the lack of finite beam and wall effects. In particular, there is close agreement between the measurements and POLAR's predicted onset for current collection and the variation with separation distance. At voltages above onset, POLAR, as MACH, underestimates the current. Some underestimate is to be expected since secondary emission is turned off in both codes. This was done to show just the ion current since the measurements seem to indicate an exotic secondary emission mechanism.

VIII. Comparisons and Discussion

Our goals in this study were to learn something about the collection of current in the wake of and orbiting body, and to evaluate the effectiveness of our computational tools for this type of problem.

There are points of both agreement and disagreement between the simulations.

All three simulations were in close agreement on the voltage threshold for current collection. This implies that for at [illegible] of parameters, our tools [illegible] contraints of [illegible] and spacecharge, or at [illegible] mixture of the two. There is [illegible] agreement on the magnitude of the [illegible] could be better. The [illegible] experiment and numerical [illegible] together in Fig 12.

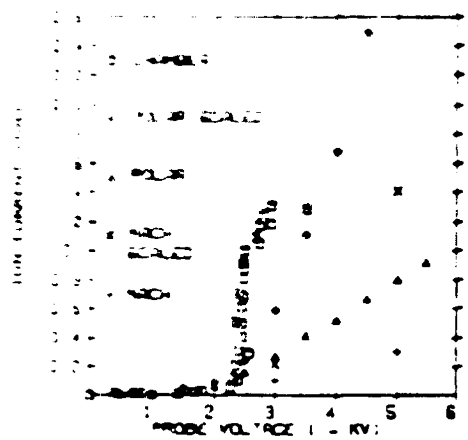

Figure 12. Simulation Currents Versus Experimental Currents

Some of the the dissagreement is certainly related to the unexpectedly high levels secondary emission discovered by the experiment. Secondary enhancement factors have been taken from the experiment, and applied to the the POLAR and MACH currents, and are displayed also in figure 12. In this case, the MACH predictions are now closer to the experiment and POLAR is too high. This is what was expected at the onset since POLAR includes a contribution from plasma beyond the extent of the experimental ion beam.

The agreement is worst on the overall morphology of the I-V curves. Although the experiment and numerical simulations agree on the turn-on inflection, the subsequent current rise is missed by both codes. Also missed was the second inflection at higher voltage where the experimental currents saturate, and the codes do not. This remains unexplained, but we can speculate on the cause of this effect. If the secondary current is carried by charged sputtered metalic ions, there would be a significant modification to the sheath spacecharge. At levels of secondary emission near the primary current, the effect would be to cancel some of the shielding Argon spacecharge and to enhance the current presuming that it was at least somewhat spacecharge limited. However, at the higher observed levels the surface charge of the probe would seem to 'come off' causing the primary ions to still enter the sheath but not find the probe. A similar effect has been noted in the operation of Hollow Cathodes in 'ignited' mode where the bulk of ionization begins to occur outside of the device in the nearby space (Wilber,1985; Cooke,1988)

Another parameter that has not been studied, but has been implicated as significant is the disk potential. The effect of this has been looked at by Katz et.al. (Katz, 1987) and found to indeed be significant.

Finally, we have used POLAR to take this issue to space. Scaling the chamber simulations Low Earth Orbit conditions while keeping the dimensionless variables described in section I constant, produced as anticipated, exactly scaled currents. This is of limited utility since an object only 40 Debye lengths ($\approx 40\,cm$) across is quite small, the scaled voltage threshold was only about $20\,Volts$, and the velocity was sub-orbital. A realistic suite of LEO condition runs has not yet been completed, but the POLAR runs so far indicate that for a Shuttle sized object (and 1/10 sized probe), the voltage threshold should be about a few hundred *Volts*.

II. References

Cooke, D.L., and I. Katz, "Ionization-Induced Instability in an Electron-Collecting Sheath", Journal of Spacecraft and Rockets Vol 25, #2, pp. 132-138, March 1988.

Katz, I., M.J.Mandell, D.E.Parks, K.Wright, N.H.Stone, and U.Samir, "The effect of Object Potentials on the Wake of a flowing Plasma" J. Appl. Phys. 62(7), Oct 1987, AFGL-TR-87-0023, 1986. ADA184038

Langmuir,I. and Blodgett,K. B.; "Currents Limited by Space Charge Between Concentric Spheres," Physical Review, 24, July, 1924.

Lilley J.R.,Jr., D.L. Cooke, G.A. Jongward, I. Katz, "POLAR Users Manual", AFGL-TR-85-0246, 1985. ADA173758

Murphy, G., and I. Katz, "The POLAR Code Wake Model: Comparison with in Situ Observations", J Geophys.Res., V94, pp. 1,450, 1989.

Parker, L.W. , "Plasmasheath-Photosheath Theory for Large Space Structures", in Space Systems and Their Interactions with the Earth's Space Environment, Prog. in Ast. and Aero. Vol.71, ed. by H.B. Garret, and C.P. Pike, 1980.

Parker, L.W., "Computation of Collisionless Steady-State Flow Past a Charged Disk", NASA CR-144159, 1976.

Tautz, M.F., D.L. Cooke, A.G. Rubin, G.K.

Yates, "Preliminary Documentation of the MACH Code", AFGL-TR-88-0035, 1987. ADA198956

Wei, R., and P.J. Wilbur, "Space-Charge-Limited Current Flow in a Spherical Double Sheath", Jounmal of Applied Physics, Vol 60, pp. 2280-2284. Oct. 1986